Review of Casimir Effect for Massless Fermions in One Dimension via a Force Operator Approach

PH3203: ADVANCED QUANTUM MECHANICS

July 11, 2025

Poluri Gowtham Sai	Nimish Sharma	Abhay Saxena
21MS220	21MS184	21MS086

Contents

Abstract

This study presents a novel force operator approach to investigate the Casimir effect mediated by massless Dirac fermions within one-dimensional systems, focusing on its applications such as carbon nanotubes. By embedding two finite square barriers in a background of one-dimensional massless Dirac fermions, we calculate the Casimir force as a function of distance between the barriers. Our approach successfully eliminates ultraviolet divergences even when considering scatterers of zero width and infinite potential strength, offering a significant improvement over traditional energy-based methods. The interaction energy and force are shown to scale with the inverse square of the distance between scatterers, consistent with classical Casimir effects but distinctly tunable via the relative spinor polarizations of the scatterers. This tunability allows for the force to range from attractive to repulsive, providing a new way to control interactions at the nanoscale. Our results also demonstrate that the one-dimensional Casimir interaction dominates over traditional van der Waals forces for charge-neutral species within these systems.

1 Introduction

The attraction between two parallel plates that are completely conducting and uncharged when they are confined in a vacuum is known as the Casimir effect. This phenomenon was first predicted by the Dutch physicist Hendrik B. G. Casimir in a 1948 publication. He defined it as the difference in pressure between two sides of a plate due to variations in the vacuum fluctuations between and within the plates.

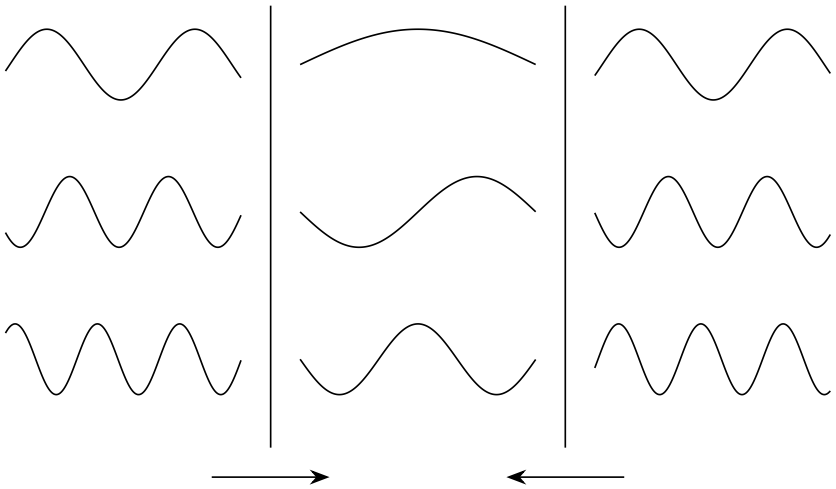

FIGURE 1: *Casimir force between two parallel plates. There is an attractive force acting on both plates because the pressure between the two is less than the pressure exerted from the outside.[source:self, LaTeX[2]]*

In his article titled 'On the attraction between two perfectly conducting plates'[2] , H.B.G Casimir presented the result that, for two perfectly conducting plates at a distance a_μ microns apart, for Force per cm^2, we find:

$$F = -\hbar c \frac{\pi^2}{240} \frac{1}{a_\mu^4} = -\frac{0.013}{a_\mu^4} dyne/cm^2 \tag{1}$$

This implies, two 1×1 plates separated by $1\mu m$ experience a force $F = -0.013 dyne$. This force is comparable to the Coulomb force on the electron in the Hydrogen atom,

thereby emphasizing the importance of Casimir interaction at an atomic level. We will understand and derive this equation in coming sections.

1.1 Zero Point Energy

Wave equation of Electric field in vacuum (E) can be given from Maxwell's Equations[4]:

$$\nabla^2 E - \frac{1}{c}\frac{\partial^2 E}{\partial t^2} = 0 \tag{2}$$

This solution of this equation can be written sum of *mode functions* [5], $\nu_m(x)$ satisfying the condition:

$$\nabla^2 \nu_m(x) = -k_m^2 \nu_m(x) \qquad (k_m^2 = \tfrac{\omega^2}{c^2})$$
$$\nabla \cdot \nu_m(x) = 0$$
$$\hat{n} \times \nu_m(x) = 0$$

Here $\hat{n}$ is the unit vector normal to the conducting surface as tangential component must vanish (Dirichlet boundary condition). Upon choosing orthonormal modes:

$$E(x,t) = \sum_m f_m(t)\nu_m(x)$$

replace in Equation (2), to get:

$$\frac{d^2}{dt^2} f_m(t) + c^2 k_m^2 f_m(t) = 0$$

Which is an equation of Harmonic Oscillator with angular frequency $\omega_m = ck_m$. Mangetic Field B will expand to similar form:

$$B(x,t) = \sum_m h_m(t) \nabla \times \nu_m(x)$$

with:

$$\frac{d}{dt} h_m(t) - c f_m(t) = 0$$

leading to:

$$\frac{d^2}{dt^2} h_m(t) + c^2 k_m^2 h_m(t) = 0$$

This analysis of normal modes shows, EM fields are nothing but infinite independent harmonic oscillators.

$$\mathcal{H} = \frac{1}{8\pi}\int (E^2 + B^2) dx$$

$$= \frac{1}{8\pi}\sum_{m,m'} f_{m'} f_m \int \nu_{m'}\nu_m dx + \frac{1}{8\pi}\sum_{m,m'} h_{m'} h_m \int (\nabla \times \nu_{m'})(\nabla \times \nu_m) dx$$

$$= \frac{1}{8\pi}\sum_i f_i^2 + k_i^2 h_i^2$$

Which is similar to Simple Harmonic Oscillator:

$$\mathcal{H}_{osc} = \sum_i \frac{1}{2}(P_i^2 + \omega_i^2 X_i^2)$$

$$P_m = \frac{-f_m(t)}{2\sqrt{\pi}}; X_m = \frac{h_m}{2c\sqrt{\pi}}$$

Upon quantization of Electromagnetic field [4], one can write the Hamiltonian as sum of Simple Harmonic Oscillator:

$$\mathcal{H} = \sum_i \hbar\omega_i(a_i^\dagger a_i + \frac{1}{2}) \tag{3}$$

where:

$$a_i^\dagger |n\rangle = \sqrt{n+1}\,|n+1\rangle \qquad \text{(creation operator)}$$

$$a_i |n\rangle = \sqrt{n}\,|n-1\rangle \qquad \text{(annihilation operator)}$$

Applying a_i on $|0\rangle$, we can write it's ground state as a:

$$a_i |0\rangle = 0$$

where, no more photons can be annihilated, as there are none. Thus, we now find expectation energy on ground state as:

$$\langle E\rangle = \langle 0|\mathcal{H}|0\rangle = \langle 0|\sum_i \hbar\omega_i(a_i^\dagger a_i + \frac{1}{2})|0\rangle = \frac{1}{2}\sum_i \hbar\omega_i = \frac{1}{2}\int_0^\infty \hbar\omega g(\omega)d\omega$$

Where $g(\omega)$ is density of the state. Hence, this is sum of many uncoupled harmonic oscillators, each with energy $\frac{1}{2}\hbar\omega$. This results in a calculation of infinite zero-point energy in any finite volume; this is one reason renormalization is needed to make sense of quantum field theories. Under ordinary conditions this infinity is not physically measurable, as it is present at each point in space. Only upon imposing boundary conditions, do we see it in effect.

1.2 Deriving Casimir force in 3D

Consider a sizable cavity with dimensions $L \times L \times L$, enclosed by conducting walls. A conducting plate is introduced at a distance R parallel to one of the xy walls, with R significantly smaller than L. We aim to compute the energy variation caused by the presence of the conducting plate at $z = R$:

$$\Delta E = E_R + E_{L-R} - E_L$$

The diagram below illustrates the setup, depicting a large cavity with a plate inserted near one end at a distance R.

The conducting walls enforce Dirichlet boundary conditions on the electromagnetic modes within the cavity, demanding the vanishing of the tangential component of the electromagnetic field. Solving the wave equation with these conditions reveals quantized values for the x, y, and z components of the wavevectors k, defined as:

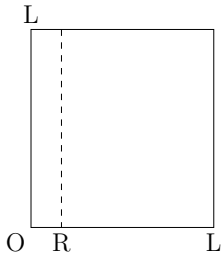

$$k_x = \frac{n_x \pi}{L}, \quad k_y = \frac{n_y \pi}{L}, \quad k_z = \frac{n_z \pi}{R}$$

In vacuum, the angular frequency ω relates to the wave number k by the speed of light c:

$$\omega = ck$$

This allows us to express the zero-point energy of the field as:

$$\langle E \rangle = \frac{1}{2}\hbar c \sum \sqrt{k_x^2 + k_y^2 + k_z^2} \tag{4}$$

Given the assumption of a large cavity ($R \ll L$), we replace the summation with an integral to obtain the energies:

$$E_L = \frac{2L^3}{\pi^3} \int\int\int_0^\infty \frac{1}{2}\hbar c \sqrt{k_x^2 + k_y^2 + k_z^2}\, dk_x\, dk_y\, dk_z$$

$$E_{L-R} = \frac{2L^2(L-R)}{\pi^3} \int\int\int_0^\infty \frac{1}{2}\hbar c \sqrt{k_x^2 + k_y^2 + k_z^2}\, dk_x\, dk_y\, dk_z$$

$$E_R = \sum_{n=0}^{\infty} \frac{2\theta_n L^2}{\pi^2} \int\int_0^\infty \frac{1}{2}\hbar c \sqrt{k_x^2 + k_y^2 + \left(\frac{n\pi}{R}\right)^2}\, dk_y\, dk_z$$

Here, $n \equiv n_z$, and θ_n is defined as 1 for $n > 0$, and $\frac{1}{2}$ for $n = 0$, reflecting the different polarization states of k. This notation simplifies the subsequent use of the Euler-Maclaurin formula.

Both the summation and integrals diverge, necessitating the introduction of a smooth cutoff function, $f(k/k_c)$, satisfying:

$$f(k/k_c) \to 1, \quad k \ll k_c$$

$$f(k/k_c) \to 0, \quad k \gg k_c$$

This is justified by the notion that each conductor has a plasma frequency $\omega_p^2 = \frac{Nq^2}{m_e \epsilon_0}$, representing the minimum oscillation frequency supported by the electrons in the conductor. Below this frequency, the conductor behaves as a reactive medium, reflecting electromagnetic waves and enforcing the discussed boundary conditions. Above the plasma frequency, the conductor becomes transparent to photons, rendering the boundary conditions invalid.

The energy difference equation now becomes:

$$\Delta E = \hbar c \frac{L^2}{\pi^2} \left[\sum_{n=0}^{\infty} \theta_n g\left(\frac{n\pi}{R}\right) - \frac{R}{\pi} \int_0^{\infty} g(k_z)\, dk_z \right]$$

where

$$g(k_z) = \int \int_0^{\infty} f\left(\frac{k}{k_c}\right) \sqrt{k_x^2 + k_y^2 + k_z^2}\, dk_x\, dk_y$$

Simplifying $g(k_z)$ through transformations, we obtain:

$$g(k_z) = \frac{\pi^4 F(n)}{4R^3}$$

where

$$F(n) = \int_{n^2}^{\infty} \sqrt{\omega} f\left(\frac{\pi\sqrt{\omega}}{Rk_c}\right)\, d\omega$$

This leads to the final expression for the energy difference:

$$\Delta E = \frac{\hbar c L^2 \pi^2}{4R^3} \left[\sum_{n=0}^{\infty} \theta_n F(n) - \int_0^{\infty} F(n)\, dn \right]$$

The difference between the summation and the integral is approximated using the Euler-Maclaurin formula:

$$\sum_{n=0}^{\infty} \theta_n F(n) - \int_0^{\infty} F(n)\, dn = -\frac{1}{12} F'(0) + \frac{1}{720} F'''(0) - \dots$$

With $F'(n)$, we find:

$$F'(n) = -2n^2 f\left(\frac{n^2\pi}{Rk_c}\right)$$

resulting in:

$$\Delta E = -\frac{\hbar c \pi^2}{720} \frac{L^2}{R^3}$$

The force per cm^2 is then determined to be:

$$F = -\frac{1}{L^2} \frac{\partial \Delta E}{\partial R} = -\frac{\hbar c}{240} \frac{\pi^2}{R^4} \tag{5}$$

This yields the desired result as initially stated.

1.3 Deriving Casimir force in 1D

Now we proceed with deriving casimir force in 1-D[8]. We model our 1-D Lattice as shown in Figure-2

We begin with taking a continuum limit, we let $N \to \infty$ and $d \to 0$. ω_r in this limit in 1-D is given by:

$$\omega_r = \frac{c\pi r}{l} \tag{6}$$

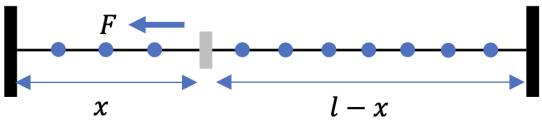

FIGURE 2: *Discrete scalar field bounded by end plates. The movable plate at distance x experiences an attractive force F towards the nearest plate.[8]*

where $r = 1, 2, 3, ...\infty$. Using Eq(4), we write the zero point energy in gap of length x:

$$\begin{aligned} U(n) &= \sum_{r=1}^{n} \frac{1}{2}\hbar\omega_r \\ U(x) &= \frac{\pi\hbar c}{2x}\sum_{r=1}^{\infty} r \end{aligned} \tag{7}$$

The zero point energy of the system is given by:

$$U(x, l) = U(x) + U(l - x) \tag{8}$$

In the limit $l >> x$, we obtain an infinite force which must be regulated using zeta function:

$$F = -\frac{dU}{dx} = \frac{\pi\hbar c}{2x^2}\sum_{r=1}^{\infty} r$$
$$1 + 2 + 3 + .. \rightarrow -\frac{1}{12}$$

Thus, we obtain the final expression for force as:

$$F = -\frac{\pi\hbar c}{24x^2} \tag{9}$$

2 Theoretical Framework

The interaction between scatterers in a one-dimensional electron gas, particularly involving massless Dirac fermions, requires an understanding of the modified quantum vacuum states.

2.1 Hamiltonian

We start off by writing the Hamiltonian for the massless Dirac fermions :

$$\left(-i\sigma_x\frac{\partial}{\partial x} + \hat{V}(x) - E\right)\Psi_k(x) = 0 \tag{10}$$

This equation is massless limit of Dirac equation, for spin half particles, referred to as Weyl equation.[6] For non-relativistic fermions, the dispersion relation is typically parabolic, and the Hamiltonian is indeed given by $H = \frac{p_x^2}{2m}$ where p_x is the momentum operator along the x direction, m is the mass of the particle and $\hbar$ is the reduced Planck's constant. For massless fermions, this dispersion relation is linear and is given by $E = v_F|\pm k|$.

The term $-i\sigma_x \frac{\partial}{\partial x}$ is used instead of $\frac{\hbar^2}{2m}\frac{\partial^2}{\partial x^2}$ (which represents the kinetic energy in the Schrödinger equation) because we are dealing with massless Dirac fermions. In the relativistic context described by the Dirac equation, the concept of mass is replaced by the Fermi velocity (v_F), and the kinetic energy term takes on a different form as $-i\sigma_x \frac{\partial}{\partial x}$. This reflects the linear dispersion relation and relativistic effects characteristic of massless Dirac fermions.

2.2 General Solution

When the potential $\hat{V}(x)$ is zero, the eigenstates of the Hamiltonian $\hat{H}_0$ are plane waves multiplied by two-dimensional spinors. Mathematically, this can be expressed as

$$\Psi_k(x) = \alpha_k \Phi_k e^{ikx} + \beta_k \Phi_{-k} e^{-ikx} \tag{11}$$

Here, α_k and β_k represent the amplitudes of the counter propagating waves in each region and $\Phi_{\pm k}$ correspond to the two possible spin states for the fermion at momentum k i.e.

$$\Phi^T_{\pm k}(x) = \frac{(1, \mp 1)}{\sqrt{2\pi}} \tag{12}$$

In this case, the z-component of the spin is quantized, and the two spin states are orthogonal. The normalization ensures that the total probability density is conserved.

For a fixed chemical potential $\mu = 0$, the energy eigenvalues(E) correspond to the eigenvalues of the Hamiltonian. In the case of massless Dirac fermions, the dispersion relation is linear, and the energy eigenvalues are given by $E = -|k|$. The negative energy states represent filled states, forming what's known as the Dirac sea with $\Phi^T_{\pm k} = (1, \mp 1)/\sqrt{2}$.

2.3 Potential

The general form of potential $\hat{V}(x)$ in Eq(10) is given by $\hat{V}(x) = V_o(x)\hat{I} + \vec{V} \cdot \vec{\sigma}$ where the second term corresponds to a vector potential acting on the spin degrees of freedom.

In order to simplify our analysis, we claim that we can only focus on the potentials for which $\vec{V}$ lies in the y-z plane. We can do so because of the following reasons :

- Gauge Transformation : The σ_x part of the potential can be eliminated by a Gauge Transformation given by $\Psi(x) \rightarrow e^{i\theta(x)\sigma_x}\Psi(x)$. We can apply the Gauge transformation to Eq(10) and carefully choose $\theta(x)$ such that σ_x cancels out, i.e. $e^{i\theta(x)\sigma_x}\sigma_x = \sigma_x e^{i\theta(x)\sigma_x}$. This essentially eliminates the σ_x part of the potential term while preserving the physical meaning of the Dirac equation.

- Backscattering : Backscattering occurs when particles are scattered backward due to the potential encountered. In terms of the wavefunction, this means a change in momentum direction. the scalar potential $V_o\vec{I}$ unlike the vector potential $\vec{V} \cdot \vec{\sigma}$ only affects the amplitude of the wavefunction at a given position, not its direction. Since it doesn't couple to the spin degree of freedom, it doesn't cause any change in the momentum direction or spin orientation of the particles. Instead, it just alters the overall magnitude of the wavefunction, essentially just scaling it by a position-dependent factor. This is why it's often disregarded in discussions regarding backscattering in the context of the Dirac equation.

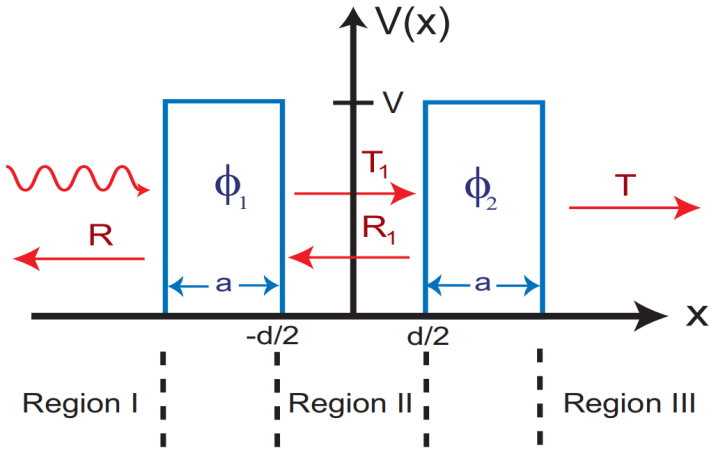

FIGURE 3: *Visualisation of potential[1]*

We consider the effects of the orientation of the potential determined by angle ϕ. Thus, a square barrier potential located between points x_1 and x_2 as show in Figure 3 is written as :

$$\hat{V}(x,\phi) = \hat{V}(\phi)\theta(x-x_1)\theta(x-x_2) \tag{13}$$

where $\hat{V}(\phi) = Ve^{i\sigma_x\phi/2}\sigma_z e^{-i\sigma_x\phi/2}$, and $\theta(x)$ is a step function.

2.4 Hellmann-Feynman Theorem

The Hellmann-Feynman theorem is a fundamental result in quantum mechanics that provides a way to calculate the derivative of the expectation value of an observable with respect to a parameter in the Hamiltonian. Mathematically, it states:

$$\left\langle \psi \middle| \frac{\partial \hat{H}(\lambda)}{\partial \lambda} \middle| \psi \right\rangle = \frac{\partial E}{\partial \lambda} \tag{14}$$

Now, in the context of studying the force on a square well scatterer, we choose the control parameter λ to be the average position of the scatterer, $\bar{x} = \frac{x_1+x_2}{2}$, where x_1 and x_2 are the positions of the ends of the square well. This choice of parameter allows us to investigate how changes in the position of the scatterer affect the energy of the system.

By taking the ground state average, we compute the expectation value of the force acting on a rigid barrier due to the square well scatterer. The ground state average represents the expectation value of the force when the system is in its lowest energy state, which is often the state of interest in many physical scenarios. In this case, it allows us to determine the force exerted on the barrier by the potential created by the square well scatterer.

3 Methodology

The methodology involves calculating the force between finite width square barriers representing scatterers, with an aim to analyze the Casimir force mediated by one-dimensional massless Dirac fermions. The approach avoids the traditional complications associated

with ultraviolet divergences, employing the Hellmann-Feynman theorem to derive expressions for the force as a function of scatterer separation.

3.1 Applying Hellmann-Feynman Theorem

We start off by applying the Hellmann-Feynman Theorem, Eq(13) for our Hamiltonian. Firstly we note that the derivative of the Hamiltonian with respect to $\bar{x}$ represents how the Hamiltonian changes as the center of the barrier potential shifts. In this case, it's given by:

$$\frac{\partial \hat{H}(\bar{x})}{\partial \bar{x}} = \frac{\partial \hat{V}(\bar{x})}{\partial \bar{x}} \tag{15}$$

We evaluate the expectation value at the edges of the square potential,i.e. $\bar{x} + \frac{a}{2}$ and $\bar{x} - \frac{a}{2}$ as shown in Figure 3. This gives us:

$$\langle \Psi(x) \mid \frac{\partial \bar{H}}{\partial \hat{x}} \mid \Psi(x) \rangle = \langle \Psi(\bar{x} + \frac{a}{2}) \mid \hat{V} \mid \Psi(\bar{x} + \frac{a}{2}) \rangle - \langle \Psi(\bar{x} - \frac{a}{2}) \mid \hat{V} \mid \Psi(\bar{x} - \frac{a}{2}) \rangle \tag{16}$$

We aim to find the total force by summing the force operator over all states, given by:

$$\hat{F} = -\frac{\partial \hat{H}}{\partial \bar{x}} \tag{17}$$

Therefore, Eq(16) gives us the difference between the pressures exerted on the right and the left sides of the barrier.

Using Eq(13) and Eq(12) and applying $\hat{V}(\phi)$ on $\Phi_{\pm k}$ gives us:

$$\hat{V}(\phi)\Phi_{\pm k} = Ve^{\pm i\phi}\Phi_{\mp k} \tag{18}$$

Applying $e^{i\sigma_x \phi/2}$ and $e^{-i\sigma_x \phi/2}$ doesn't affect $\Phi_{\pm k}$ as it just represents the rotation in x axis by an angle $\pm\phi/2$ which is perpendicular to y-z plane. Action of σ_z flips the spin state changing Φ_k to Φ_{-k}. In order to see the action of $\hat{V}(\phi)$ in its full glory, we can expand the exponential term in matrix format and then apply it.

Now we can finally calculate $\left\langle \Psi(x) \middle| \hat{V}(\phi) \middle| \Psi(x) \right\rangle$ using Eq(11), Eq(12) and Eq(18) as demonstrated below:

$$\begin{aligned}
\hat{V}(\phi)|\Psi(x)\rangle &= V(\alpha_k e^{i(kx+\phi)}\Phi_{-k} + \beta_k e^{-i(kx+\phi)}\Phi_k) \\
Note : \langle \Psi(x)| &= \alpha_k^* e^{-ikx}(\Phi_k^*)^T + \beta_k^* e^{ikx}(\Phi_{-k}^*)^T \\
\left\langle \Psi(x) \middle| \hat{V}(\phi) \middle| \Psi(x) \right\rangle &= \frac{V}{2\pi}(0 + \alpha_k^*\beta_k e^{-i(2kx+\phi)} + \alpha_k\beta_k^* e^{i(2kx+\phi)} + 0) \\
\left\langle \Psi(x) \middle| \hat{V}(\phi) \middle| \Psi(x) \right\rangle &= \frac{V}{\pi}\left(\frac{\alpha_k\beta_k^* e^{i(2kx+\phi)} + \alpha_k^*\beta_k e^{-i(2kx+\phi)}}{2}\right) \\
\left\langle \Psi(x) \middle| \hat{V}(\phi) \middle| \Psi(x) \right\rangle &= \frac{V}{\pi} Re\left[\alpha_k\beta_k^* e^{i(2kx+\phi)}\right]
\end{aligned} \tag{19}$$

3.2 Transfer Matrices

We shall define tranfer matrix and then use Eq(19) to obtain α_k and β_k as below:

$$\Psi(x_2) = T\Psi(x_1) \tag{20}$$

This tranfser matrix helps us define how the wavefunction evolves over the barrier since x_1 and x_2 were defined to be the barrier boundaries. We calculate T by integrating Eq(10) from x_1 to x_2.

$$\partial_x \Psi(x) = i\sigma_x^{-1}(E - \hat{V})\Psi(x)$$
$$\int_{x_1}^{x_2} \frac{1}{\Psi(x)}\, d\Psi(x) = \int_{x_1}^{x_2} i\sigma_x(E - \hat{V})\, dx$$

We used the fact that $\sigma_x^{-1} = \sigma_x$. Finally, Integrating, we get:

$$\Psi(x_2) = exp\left(i\int_{x_1}^{x_2} \sigma_x(E - \hat{V})\, dx)\right)\Psi(x_1)$$

The presence of a non-commuting operator, particularly if $\hat{V}(x)$ varies with x, requires the use of a path-ordered exponential. This is noted as P_x, indicating that the terms in the exponential must be ordered according to their position along the path from x_1 to x_2. The exact form of the transfer matrix T becomes:

$$T = P_x exp\left(i\int_{x_1}^{x_2} \sigma_x(E - \hat{V})\, dx)\right) \tag{21}$$

Now we proceed by calculating T. In our problem, we have $\vec{V} = (0, sin(\phi), cos(\phi)) = \sigma_y sin(\phi) + \sigma_z cos(\phi)$ which defines a potential in the y-z plane and is independent of x. Hence, T becomes:

$$T = P_x exp\left(i\sigma_x(E - \vec{V})(x_2 - x_1)\right)$$

since $x_2 - x_1 = a$,

$$T = exp\left(i\sigma_x \begin{bmatrix} E - Vcos(\phi) & -iVsin(\phi) \\ iVsin(\phi) & E + Vcos(\phi) \end{bmatrix} a\right)$$
$$T = exp\left(ia \begin{bmatrix} iVsin(\phi) & E + Vcos(\phi) \\ E - Vcos(\phi) & -iVsin(\phi) \end{bmatrix}\right)$$
$$T = exp\left(\begin{bmatrix} -aVsin(\phi) & ia(E + Vcos(\phi)) \\ ia(E - Vcos(\phi)) & aVsin(\phi) \end{bmatrix}\right)$$

Now, inorder to exponentiate the matrix, we need to diagonalise it and then expo-

nentiate. We find its eigenvalues as $\pm iaq$ where $q = \sqrt{E^2 - V^2}$. Therefore $T = S^{-1}DS$.

$$S = \begin{bmatrix} -\frac{q - iVsin(\phi)}{E - Vcos(\phi)} & \frac{q + iVsin(\phi)}{E - Vcos(\phi)} \\ 1 & 1 \end{bmatrix}$$

$$D = \begin{bmatrix} -iaq & 0 \\ 0 & iaq \end{bmatrix}$$

$$S^{-1} = \begin{bmatrix} -\frac{E - Vcos(\phi)}{2q} & \frac{1}{2}\left(1 + \frac{iVsin(\phi)}{q}\right) \\ \frac{E - Vcos(\phi)}{2q} & \frac{1}{2}\left(1 - \frac{iVsin(\phi)}{q}\right) \end{bmatrix}$$

$$e^D = \begin{bmatrix} e^{-iaq} & 1 \\ 1 & e^{iaq} \end{bmatrix}$$

Now, after rigorous calculation, we get $e^T = S^{-1}e^D S$ as the following:

$$T = \frac{e^{-iaq}}{2q} \begin{bmatrix} iVe^{2iaq}sin(\phi) + qe^{2iaq} + q - iVsin(\phi) & -iVe^{2iaq}sin(\phi) + qe^{2iaq} - q + iVsin(\phi) \\ i(Ve^{2iaq}sin(\phi) - iqe^{2iaq} + iq - Vsin(\phi)) & i(Ve^{2iaq}sin(\phi) - iqe^{2iaq} - iq - Vsin(\phi)) \end{bmatrix}$$

Using Sympy Library[3] this simplifies further to:

```
from sympy import *

sigma_x = Matrix([[0, 1], [1, 0]])
sigma_y = Matrix([[0, -I], [I, 0]])
sigma_z = Matrix([[1, 0], [0, -1]])
identity = Matrix([[1, 0], [0, 1]])

# Defining V
a, d = symbols('a d', positive=True)
V, x, phi = symbols('V x phi')

# V inside barrier range
Vt = (V*exp(I*sigma_x*phi/2)*sigma_z*exp(-I*sigma_x*phi/2))
    .rewrite(sin).trigsimp()

power = (I*sigma_x*(-k*identity-Vt)*(x2 - x1)).rewrite(sin).trigsimp()

# Defining original T from integral
T = exp(power).subs(sqrt(V**2 - k**2), I*q)
.subs(k, sqrt(V**2 + q**2)).simplify().subs(sqrt(-q**2), I*q)

#simplify T to match with Tal
T.applyfunc(lambda x: x.subs(exp(2*I*a*q), cos(2*a*q) + I*sin(2*a*q))
    .subs(exp(-I*a*q), cos(-a*q) + I*sin(-a*q)).expand().trigsimp())

# Alternate T for the transfer matrix for negative energy states
x_vec = Matrix([1, 0, 0])
Vt_vec = V * Matrix([0, sin(phi), cos(phi)])

cp = x_vec.cross(Vt_vec)

Tal = cos(q*a)*identity -
    (I*sigma_x*k - sigma_x*cp[0] - sigma_y*cp[1] - sigma_z*cp[2])*sin(q*a)/q

# Matrices T and Tal come out to be same
```

$$T = \begin{bmatrix} \frac{qcos(qa) + Vsin(\phi)sin(qa)}{q} & \frac{-isin(qa)(E - Vcos(\phi))}{q} \\ \frac{-isin(qa)(E + Vcos(\phi))}{q} & \frac{qcos(qa) - Vsin(\phi)sin(qa)}{q} \end{bmatrix}$$

$$T = \begin{bmatrix} \cos(qa) & 0 \\ 0 & \cos(qa) \end{bmatrix} - \frac{\sin(qa)}{q}\left(\begin{bmatrix} 0 & iE \\ iE & 0 \end{bmatrix} - \begin{bmatrix} 0 & iV\cos(\phi) \\ -iV\cos(\phi) & 0 \end{bmatrix} - \begin{bmatrix} V\sin(\phi) & 0 \\ 0 & -V\sin(\phi) \end{bmatrix}\right)$$

Using Pauli Matrices, this further simplifies to:

$$\begin{aligned} T &= cos(qa) - \frac{sin(qa)}{q}(i\sigma_x E + V cos(\phi)\sigma_y - V sin(\phi)\sigma_z) \\ T &= cos(qa) - \frac{i\sigma_x E - \vec{\sigma}\cdot(\hat{x}\times\vec{V})}{q} sin(qa) \end{aligned} \tag{22}$$

Giving us the final T operator. This operator given by Equation (20) is such That,

$$T(Ae^{ikx_1}|+\rangle + Be^{-ikx_1}|-\rangle) = Ce^{ikx_2}|+\rangle + De^{-ikx_2}|-\rangle$$

with:

$$a = x_2 - x_1$$

Hence to find the final matrix, each element can be calculated as:

$$T_{11} = \langle +|T|+\rangle$$

$$T_{12} = \langle -|T|+\rangle$$

$$T_{21} = \langle +|T|-\rangle$$

$$T_{22} = \langle -|T|-\rangle$$

giving us Transfer matrix as:

$$\mathcal{T} = \begin{bmatrix} \left(\frac{ik\sin(aq)}{q} + \cos(aq)\right)e^{-ik(-x_1+x_2)} & \frac{Ve^{-i\phi}e^{-ik(x_1+x_2)}\sin(aq)}{q} \\ \frac{Ve^{i\phi}e^{-ik(-x_1-x_2)}\sin(aq)}{q} & \left(-\frac{ik\sin(aq)}{q} + \cos(aq)\right)e^{-ik(x_1-x_2)} \end{bmatrix} \tag{23}$$

3.3 Scattering Matrix

3.3.1 Single Barrier

We can now find out the scattering matrix from our transfer matrix using the following result. Using S matrix we can calculate t and r which are the transmitted and reflected amplitudes. given :

for S matrix-

$$C = S_{11}A + S_{12}D$$

$$B = S_{21}A + S_{22}D$$

for T matrix-

$$C = T_{11}A + T_{12}B$$

$$D = T_{21}A + T_{22}B$$

hence giving us final S matrix as:

$$\mathcal{S} = \begin{pmatrix} T_{11} - \frac{T_{21}T_{12}}{T_{22}} & \frac{T_{12}}{T_{22}} \\ -\frac{T_{21}}{T_{22}} & \frac{1}{T_{22}} \end{pmatrix} \tag{24}$$

Apply Equation (24) to Transfer Matrix (23) to get $\mathcal{S}$ as:

$$\mathcal{S} = \begin{bmatrix} -\frac{qe^{-iak}}{ik\sin(aq) - q\cos(aq)} & \frac{Ve^{-i(2kx_2+\phi)}\sin(aq)}{-ik\sin(aq)+q\cos(aq)} \\ -\frac{Ve^{i(2kx_1+\phi)}\sin(aq)}{ik\sin(aq)-q\cos(aq)} & -\frac{qe^{-iak}}{ik\sin(aq)-q\cos(aq)} \end{bmatrix} \tag{25}$$

Where :

$$\frac{-V^2\sin^2(aq) + k^2\sin^2(aq) + q^2\cos^2(aq)}{q^2} = 1 \qquad \text{(determinant of } \mathcal{T}\text{)}$$

replace $cos(qa) = cosh(\lambda a)$ as $\lambda = -iq$, and similarily for $sin(qa)$ to get:

$$\mathcal{S} = \begin{bmatrix} -\frac{qe^{-iak}}{-k\sinh(a\lambda)-q\cosh(a\lambda)} & \frac{iVe^{-i(2kx_2+\phi)}\sinh(a\lambda)}{k\sinh(a\lambda)+q\cosh(a\lambda)} \\ -\frac{iVe^{i(2kx_1+\phi)}\sinh(a\lambda)}{-k\sinh(a\lambda)-q\cosh(a\lambda)} & -\frac{qe^{-iak}}{-k\sinh(a\lambda)-q\cosh(a\lambda)} \end{bmatrix} \tag{26}$$

We can now define the matrix S_1 which represents the unitary matrix for a single square barrier:

$$S_1 = \begin{bmatrix} te^{-ika} & re^{-i(2kx_2+\phi)} \\ re^{i(2kx_1+\phi)} & te^{-ika} \end{bmatrix} \tag{27}$$

where the transmission and reflection coefficients can be found from S, Eq(24) and are parametarized by:

$$\begin{aligned} t &= \frac{q}{k\sinh(a\lambda)+q\cosh(a\lambda)} = \tau e^{i\eta} \\ r &= \frac{iV\sinh(a\lambda)}{k\sinh(a\lambda)+q\cosh(a\lambda)} = i\sqrt{1-\tau^2}e^{i\eta} \end{aligned} \tag{28}$$

where,

$$\begin{aligned} \tau &= \frac{\lambda}{(V^2 cosh^2(\lambda a) - k^2)^{1/2}} \\ \eta &= tan^{-1}\left(\frac{k tanh\lambda a}{\lambda}\right) \\ \lambda &= -iq = \sqrt{V^2 - k^2} \end{aligned} \tag{29}$$

We can see that for a single barrier, the forces from the left and right cancels out due to the partices. Whereas in a double barrier case, a net force will arise from multiple reflections between two barriers.

3.3.2 Double Barrier

We can write the scattering matrix for both the barriers:

$$\begin{aligned} \begin{bmatrix} \zeta_{cav_R} \\ \Phi_{out} \end{bmatrix} &= S_1 \begin{bmatrix} \psi_{in} \\ \zeta_{cav_L} \end{bmatrix} \\ \begin{bmatrix} \psi_{out} \\ \zeta_{cav_L} \end{bmatrix} &= S_2 \begin{bmatrix} \zeta_{cav_R} \\ \Phi_{in} \end{bmatrix} \end{aligned} \tag{30}$$

Where S_1 and S_2 can be found from Eq(27). From Eq(30), we can obtain the generalized scattering matrix for a double barrier can be given by:

$$\begin{aligned} S_{tot} &= \begin{bmatrix} T & Re^{i\phi_1} \\ Re^{-i\phi_2} & T \end{bmatrix} \\ \Psi_{out} &= S_{tot}\Psi_{in} \end{aligned} \tag{31}$$

We can now also calculate Cavity Matrix which is scattering matrix inside the cavity between the two barriers:

$$\begin{bmatrix} \zeta_{cav_R} \\ \zeta_{cav_L} \end{bmatrix} = \begin{bmatrix} T_1 & R_1^{'} \\ R_1 & T_1^{'} \end{bmatrix} \begin{bmatrix} \psi_{in} \\ \Phi_{in} \end{bmatrix} \tag{32}$$

We can calculate T now for the double barrier. We know that the phase accumulated over transmission across barrier 1 and 2 is given by $e^{i\phi_1}$ and $e^{i\phi_2}$ respectively. Phase accumulated while travelling distance d between the barriers is given by e^{ikd}. So calculating :

$$T_{tot} = \frac{t^2}{1-r^2e^{i\nu}}, R_{tot} = re^{-ik(2a+d)}\left(1 + \frac{t^2e^{i(2ka+\nu)}}{1-r^2e^{i\nu}}\right) \tag{33}$$

where $\nu = 2kd + \delta\phi$ and $\delta\phi = \phi_2 - \phi_1$. Similarly, now we can use Eq(32) to write T_1 and R_1 as given in Fig(3):

$$\begin{aligned} T_1 &= \frac{t}{1-r^2e^{i\nu}} \\ R_1 &= \frac{rte^{i(kd+\phi_2)}}{1-r^2e^{i\nu}} \end{aligned} \tag{34}$$

The coefficients for the waves incoming from the left (R_1 and T_1), and the ones incoming from the right ($R_1^{'}$ and $T_1^{'}$) are related by $R_1^{'} = R_1 e^{-i(\phi_1+\phi_2)}$ and $T_1^{'} = T_1$.

3.4 Force Calculation

Now we proceed with calculating force between the barriers, using Eq(19). In order to proceed, we now divide the system into 3 regions, as shown in Figure(3) and we define the wavefunctions satisfying the Dirac Equation(10) in each of the regions as follows:

$$\begin{aligned}\Psi_I &= A_1\Phi_k e^{ikx} + A_2\Phi_{-k}e^{-ikx}\\ \Psi_{II} &= B_1\Phi_k e^{ikx} + B_2\Phi_{-k}e^{-ikx}\\ \Psi_{III} &= C_1\Phi_k e^{ikx} + C_2\Phi_{-k}e^{-ikx}\end{aligned} \tag{35}$$

Now we use Eq()19 to calculate force at 4 points, i.e. 4 edges of the barriers in the following fashion:

$$\begin{aligned}\left\langle \Psi_I\left(-a-\frac{d}{2}\right)\middle|\hat{V}(\phi_1)\middle|\Psi_I\left(-a-\frac{d}{2}\right)\right\rangle &= \frac{V}{\pi}Re\left[A_1A_2^* e^{i(2k(-a-\frac{d}{2})+\phi_1)}\right]\\ \left\langle \Psi_{II}\left(-\frac{d}{2}\right)\middle|\hat{V}(\phi_1)\middle|\Psi_{II}\left(-\frac{d}{2}\right)\right\rangle &= \frac{V}{\pi}Re\left[B_1B_2^* e^{i(2k(-\frac{d}{2})+\phi_1)}\right]\\ \left\langle \Psi_{II}\left(\frac{d}{2}\right)\middle|\hat{V}(\phi_2)\middle|\Psi_{II}\left(\frac{d}{2}\right)\right\rangle &= \frac{V}{\pi}Re\left[B_1B_2^* e^{i(2k(\frac{d}{2})+\phi_2)}\right]\\ \left\langle \Psi_{III}\left(a+\frac{d}{2}\right)\middle|\hat{V}(\phi_2)\middle|\Psi_{III}\left(a+\frac{d}{2}\right)\right\rangle &= \frac{V}{\pi}Re\left[A_1A_2^* e^{i(2k(a+\frac{d}{2})+\phi_2)}\right]\end{aligned}$$

We employ our scattering matrices to find out A_is, B_is, C_is. Next we add the two attractive forces at $-a-\frac{d}{2}$ and $a+\frac{d}{d}$ and subtract the two repulsive forces due to reflections at $-\frac{d}{2}$ and $\frac{d}{2}$. Summing it over all possible energy modes depending on k gives us the following result:

$$F = -2V\int_0^\infty \frac{dk}{2\pi}Re\left[Re^{ik(d+2a)} - R_1T_1^* e^{-i(kd+\phi_2)}(1+e^{i\nu})\right] \tag{36}$$

Here we see that the the first term in the integral represents the exterior modes pushing the two barriers inwards while the second term accounts for the modes confined in the cavity pushing the two barriers apart. When incoming waves arriving at high energies will be completely transmitted for finite barriers, hence the integral will converge even in the sharp a $\to$ 0 barrier limit, with Γ = Va fixed (where Γ is essentially the "barrier strength").

We can compute the Casimir force for hard-wall boundary conditions by setting the limits of infinite barrier strength $\Gamma \to \infty$ and zero width $a \to 0$, hence enforcing a vanishing current at the boundaries. Here as we are multiplying V into the integral we will keep terms of $\mathcal{O}(\frac{k}{V})$. On evulating the integral further we see that it comes out to be:

$$F = 2\int_0^\infty \frac{dk}{2\pi}\left(k - \frac{2k\tau^2}{|1+(1-\tau^2)e^{i(\nu+2\eta)}|^2}\right) \tag{37}$$

We see that the term in the bracket rapidly oscillating as a function of k exhibiting resonances arising from the quantized nodes between the boundaries. We can represent these resonances as dirac delta functions so as to constrain our k integration:

$$\lim_{\tau\to 0}\frac{\tau^2}{|1+(1-\tau^2)e^{i(\nu+2\eta)}|^2} = \lim_{\tau\to 0}\frac{\tau^2}{1+2(1-\tau^2)\cos\nu+(1-\tau^2)^2}$$

Here we have taken $\eta \to 0$ for infinite potential barrier strength. We see that the for the $\tau \to 0$ limit, the expression is valid only if we have $\cos\nu = -1$. This would require $\nu = 2n\pi + \pi$ and hence k can only take values in the form of $k_n = \frac{\pi}{d}\left(n + \frac{1}{2}(1-\frac{\delta\phi}{\pi})\right)$. So,

$$\lim_{\tau\to 0}\frac{\tau^2}{|1+(1-\tau^2)e^{i(\nu+2\eta)}|^2} = \frac{\pi}{2d}\sum_{n=0}^{\infty}\delta(k-k_n) \tag{38}$$

Note that $\delta\phi$ is the difference in spinor polarizations of the two scattering potentials and $\delta\phi = 2\pi n$ denotes the situation of identical scattering. An incoming wave satisfying the resonance condition in Eq(38) will get fully transmitted through the two-barrier system while the modes in between the barriers, will get fully reflected resulting in the appropriate quantization condition. Finally we can rewrite the integral in Eq(36) as:

$$\begin{aligned} F &= 2\int_0^\infty \frac{dk}{2\pi} k \left(1 - \frac{\pi}{d}\sum_{n=0}^{\infty}\delta(k-k_n)\right) \\ F &= \int_0^\infty \frac{kdk}{\pi} - \frac{1}{d}\int_0^\infty k\sum_{n=0}^{\infty}\delta(k-k_n)dk \\ F &= \int_0^\infty \frac{kdk}{\pi} - \frac{1}{d}\sum_{n=0}^{\infty} k_n \end{aligned} \tag{39}$$

We can compute the Casimir force in Eq(39) by applying the generalized Abel-Plana formula,

$$\int_0^\infty tdt - \sum_{n=0}^{\infty}(n+\beta) = -\int_0^\infty tdt \left(\frac{\sinh 2\pi t}{\cos 2\pi\beta - \cosh 2\pi t} + 1\right) \tag{40}$$

Using Eq(40) we obtain the the casimir force between the two barriers in the $\Gamma \to \infty$ limit as:

$$F = -\frac{\pi}{24d^2}\left[1 - 3\left(\frac{\delta\phi}{\pi}\right)^2\right] \tag{41}$$

in $-\pi \leq \delta\phi < \pi$ following which it is periodic with period 2π. Similarly we can also obtain the force between two scatterers of finite height and width. In the small barrier strength limit ($\Gamma \ll 1$) the force will come out to be as:

$$F = -\frac{\Gamma^2 \cos\delta\phi}{2\pi d^2}\left[1 + \mathcal{O}\left(\frac{a}{d}\right)\right] \tag{42}$$

4 Results

On observing Eq(41) and Eq(42) we can see that the periodic nature of both forces is similar and can see that the system will exhibit the respective attractive or repulsive Casimir forces in both hard wall and small barrier strength limits.

A plot of the forces (scaled appropriately as shown in the graph) in Eq(41) and Eq(42) in the limits of $\Gamma \to \infty$ and $\Gamma \ll 1$ respectively for $a \to 0$ against $\delta\phi$ (relative spinor polarization) is shown in Fig(4) below. The solid and dashed lines represent the forces in hard and small barrier strength limits respectively. In order to compare the forces we have rescaled the magnitude of the force in $\Gamma \ll 1$ limit to $\Gamma = 1/2$.

In the limit $d \ll a$,the scaling of force with distance follows a universal $1/d^2$ dependence, and there's a consistent ratio of $1/2$ between the strengths of repulsive and attractive forces for massless one-dimensional fluctuating fields. As the range of potentials approaches the separation between them, the first-order correction arising from the shape of the scatterer scales proportionally to $\delta F/F \sim a/d$ as described in Eq(42). This behavior is akin to a multipole expansion in electrostatic interactions.

We can express the relative orientation as $\delta\phi = \cos^{-1}(\frac{\vec{V_1}\cdot\vec{V_2}}{|\vec{V_1}|\cdot|\vec{V_2}|})$. When the two are aligned as $\delta\phi = 2\pi n$ we get $F = -\pi/24d^2$Eq(9) yielding an attractive Casimir force as was obtained in this paper[7]. When the relative polarization of the defect potentials is antiparallel as $\delta\phi = (2n+1)\pi$, it yield a repulsive force of $F = \pi/12d^2$. In our calculation, the magnitude and sign of the force varies as a function of the relative polarization of two scatters at a fixed distance. As shown in Fig(4) this behavior occurs for both finite barriers and hard-wall boundaries.

The distinctive cusps observed in Fig(4) at odd multiples of n arise from a summation over discrete energy levels $E_n(\delta\phi)$. These energy bands, as depicted in the k_n values in Eq(38), intersect the zero-energy point at $\delta\phi = (2n+1)\pi$ as illustrated in Fig(5). At a constant chemical potential, with negative-energy states of the Dirac sea filled, there's a transition of one state within each 2π periodic region, marked by dotted vertical lines in Fig(5). Consequently, the force undergoes a sudden change in slope as seen in Fig(4) at the points where there's a jump in the number of occupied energy levels. However, when the barrier strength is finite, these cusps in the force disappear. The resonance condition, leading

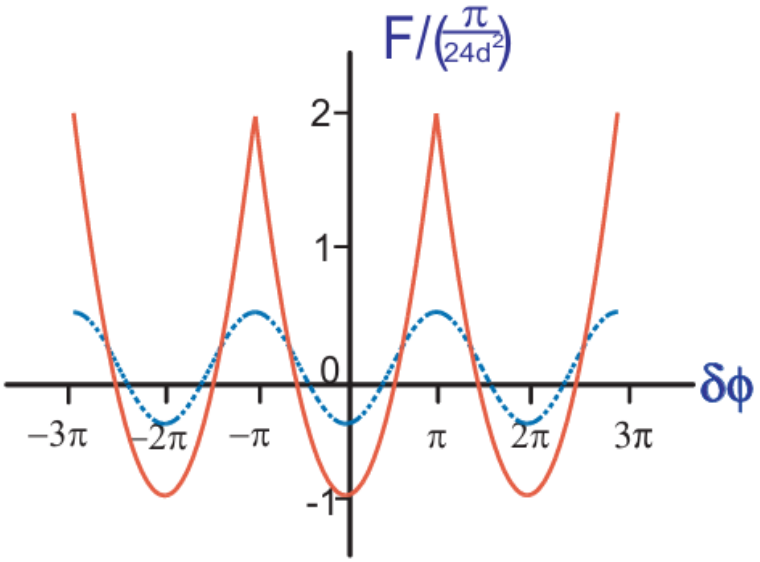

FIGURE 4: $F/\frac{\pi}{24d^2}$ *vs* $\delta\phi$ *[source:[1]]*

to quantized states between the barriers, holds true only for hard-wall boundaries. It's worth noting that energy states between finite barriers exhibit a continuous spectrum.

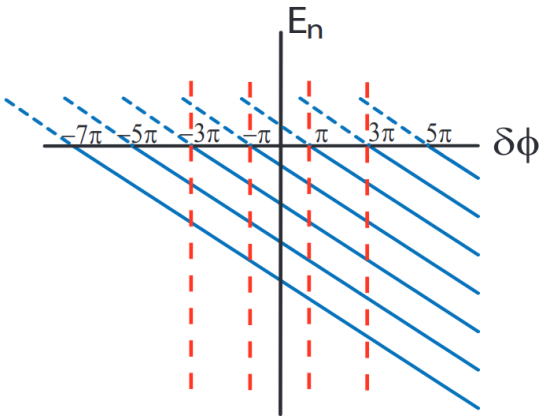

FIGURE 5: E_n *vs* $\delta\phi$ *[1]*

5 Discussion

We can see that Eq(41) can be implemented in 1-D systems such as carbon nanotubes. This force along with appropriate dimensional factors yield an interaction energy of $E_c = -\frac{\pi\hbar\nu_F}{24d}$ which gives us an energy of 1.4meV at d = 50nm. This follows the same spatial scaling as the Coulomb interaction but its value is only 5% to that of Coulomb interaction. This elaborates that for charge-neutral dipoles, whose electrostatic interactions scale as $E_d \sim p^2/d^3$, the Casimir interaction dominates in the far field, where d is much larger than 5s, indicating a strong influence of Casimir forces over electrostatic forces in specific configurations of carbon nanotubes and potentially similar one-dimensional systems.

The study marks a significant advancement in our understanding of quantum fluctuation-induced forces in low-dimensional systems. The ability to modulate the Casimir force through scatterer properties opens new avenues in the design and manipulation of nano-scale devices.

6 Conclusion

Hence, a new force operator approach was introduced to calculate the Casimir effect, revealing the fluctuation-induced force between two finite square barriers mediated by massless Dirac fermions in one dimension. This approach demonstrated that the Casimir force, which scales inversely with the square of the distance, can be adjusted from attractive to repulsive depending on the relative spinor polarizations of the scattering potentials.

References

[1] D. Zhabinskaya, J. M. Kinder, and E. J. Mele. Casimir effect for massless fermions in one dimension: A force-operator approach. *Physical Review A*, 78(6), Dec. 2008.

[2] H. B. G. Casimir. On the attraction between two perfectly conducting plates. *Indag. Math.*, 10(4):261–263, 1948.

[3] A. Meurer, C. P. Smith, M. Paprocki, O. Čertík, S. B. Kirpichev, M. Rocklin, A. Kumar, S. Ivanov, J. K. Moore, S. Singh, T. Rathnayake, S. Vig, B. E. Granger, R. P. Muller, F. Bonazzi, H. Gupta, S. Vats, F. Johansson, F. Pedregosa, M. J. Curry, A. R. Terrel, v. Roučka, A. Saboo, I. Fernando, S. Kulal, R. Cimrman, and A. Scopatz. Sympy: symbolic computing in python. *PeerJ Computer Science*, 3:e103, Jan. 2017.

[4] Wikipedia contributors. Quantization of the electromagnetic field — Wikipedia, the free encyclopedia, 2024. [Online; accessed 6-May-2024].

[5] Doron Cohen. Lecture notes in quantum mechanics, 2018.

[6] Wikipedia contributors. Weyl equation — Wikipedia, the free encyclopedia, 2023. [Online; accessed 5-May-2024].

[7] P. Sundberg and R. Jaffe. The casimir effect for fermions in one dimension. *Annals of Physics*, 309(2):442–458, Feb. 2004.

[8] Eduardo Flores, C. Ireland, N. Jamhour, V. Lasasso, N. Kurth, and M. Leinbach. Casimir force in discrete scalar fields i: 1d and 2d cases, 2023.